Shivdev Shahi

CHARACTERIZATION OF TRANSITIONAL STRESS CONCENTRATIONS IN MOLAR AND PREMOLAR IMPLANTS MODELLED AS HEMISPHERICAL SHELLS UNDER UNIAXIAL PRESSURE USING SETH'S TRANSITION THEORY

KARAKTERIZACIJA KONCENTRACIJE PRELAZNIH NAPONA U MOLARNIM I PREMOLARNIM IMPLANTIMA MODELIRANIH U OBLIKU POLUSFERNIH LJUSAKA POD DEJSTVOM JEDNOOSNOG PRITISKA PRIMENOM TEORIJE PRELAZNIH NAPONA SETA

Originalni naučni rad / Original scientific paper
UDK /UDC:
Rad primljen / Paper received: 24.12.2021

Adresa autora / Author's address:
UIS, Chandigarh University, India
email: shivdevshahi93@gmail.com

Keywords
- titanium
- zirconia
- hydroxyapatite
- implants
- stresses

Ključne reči
- titanijum
- cirkonijum
- hidroksiapatit
- implanti
- naponi

Abstract

In this paper, elastic-plastic transition stresses have been analytically characterized in titanium and zirconia based crowns of dental implants. The crown of the implant is modelled in the form of a hemispherical shell which possesses transversely isotropic material behaviour. Seth's transition theory has been implemented to model the elastic-plastic stress state. The hemispherical shell so modelled is subjected to external pressure to analyse the state of compression. The results for titanium and zirconia based implant are compared with hydroxyapatite (HAP), $Ca_{10}(PO_4)_6(OH)_2$, mineral present in the enamel and dentine of molars and premolars. Elastic stiffness constants for these are taken from the available literature, and obtained using ultrasonic resonance spectroscopy, a non-destructive technique of obtaining stiffness constants. Radial and circumferential stresses are obtained for radii ratios which can handle any type of dataset for crown thicknesses.

Izvod

U radu su analitički okarakterisani elastoplastični prelazni naponi u krunama zubnih implantata na bazi titanijuma i cirkonijuma. Kruna implanta se modelira u obliku polusferne ljuske koja ima transverzalno izotropno ponašanje materijala. Setova teorija prelaznih napona je implementirana za modeliranje elastoplastičnog stanja napona. Ovaj model polusferne ljuske je podvrgnut spoljašnjem pritisku radi analize stanja pritiska. Rezultati dobijeni za implante na bazi titana i cirkonijuma su upoređeni sa mineralom hidroksiapatit (HAP) - $Ca_{10}(PO_4)_6(OH)_2$ koji je prisutan u gleđi i dentinu molara i premolara. Konstante krutosti u elastičnom području su uzete iz dostupne literature, i dobijene su korišćenjem ultrazvučne rezonantne spektroskopije, tj. metodom ispitivanja bez razaranja. Radijalni i obimski naponi su dobijeni za odnose poluprečnika, koji mogu da zadovolje bilo koju vrstu skupa podataka za odgovarajuće debljine krunica.

INTRODUCTION

Stresses that must sustain the human masticatory system originate in the intermaxillary contact points and propagate through the dentin and enamel, /16/. Dental enamel is the hardest tissue in the human body which protects reliably a tooth from mechanical loading and aberration. It is a highly mineralised substance which contains ~ 96 % apatite by weight, /4/. One of the most important crystals that comprise dental enamel is hydroxyapatite (HAP), given by chemical formula $Ca_{10}(PO_4)_6(OH)_2$. According to early works, it has been concluded that dental enamel exhibits low ability to deformation prior to failure at ultimate compressive strength ~ 100-400 MPa, /19, 29, 30/. Human dentine is the internal structural bulk of the tooth below the enamel. Dentin is likewise a biological compound formed by ~ 50 % carbonated apatite mineral. As a stereotype, dentine is also characterized as a brittle substance, but it was recently shown that human dentine can demonstrate high elastic and plastic limits at ultimate compressive strengths ~ 800 MPa, /11, 13, 36/. Zirconia has been considered as a wear resistant and osteoconductive ceramic, highly suitable for making stress bearing crowns of dental implants. Various properties, namely, less inflammatory response, compatibility of zirconia in contact with gum tissues, lower plaque retention, and highly aesthetic toothlike colouration has made zirconia a suitable alternative to titanium implants, /2, 5, 20/. The production of ceramic dental implants have improved in past few years, /6, 21/. The yttria-stabilized tetragonal zirconia polycrystal, popularly known as Y-TZP has been a preference for some years now, having highest fracture strength /9, 10, 15, 31/. It was further confirmed that zirconia is highly flexible in all directions of the lattice plane, /17/. The Poisson ratio obtained i.e., from 0.16 to 0.31 also indicates high anisotropy. The stiffness constants so obtained will also be used in this paper for determination of elastic-plastic transitional stresses.

This paper concerns with investigation of elastic plastic transition stress in zirconia based crowns of ceramic dental implants, further comparing the results with stresses in titanium based implants. The paper also checks the similarities between the implants and human tooth enamel and dentine using Seth's transition theory. The crowns are modelled as spherical shells exhibiting transversely isotropic macrostructural symmetry. Equations for modelling spherical shells made of isotropic materials are available in most standard textbooks /3, 8, 12, 14, 18, 35/. The concept of generalised strain measures and transition theory, /22, 23/, has been applied to find elastic-plastic stresses in various problems by solving nonlinear differential equations at the transition points. Elastic-plastic transitional stresses in human tooth enamel and dentine have successfully been calculated using this theory, /25/. The results for hydroxyapatite (HAP) - $Ca_{10}(PO_4)_6(OH)_2$, which structures 95 % of enamel and 50 % of dentine by weight, are also obtained for a comparative analysis. The theory has been used to solve various problems of stress and strain determination in structures modelled in the form of discs and shells, /26, 27, 32, 33, 34/. All these problems are based on the recognition of the transition state as separate state.

GOVERNING EQUATIONS

A spherical shell with constant thickness having internal radius defined as 'a' and external radius as 'b' under uniaxial external pressure p. The external pressure acts radially to simulate the state of axial compression. Figure 1 represents the crown part of the implant that is being modelled.

Figure 1. Structure of crown part of the implant..

Displacement coordinates: in terms of spherical coordinates (r, θ, ϕ) the components of displacement are considered as:

$$u = r(1-\beta)\ ;\quad v = 0\ , \tag{1}$$

where: β is position function which depends on radius only. Seth /22-24/ gave the generalised components of strain as:

$$e_{rr} = \frac{1}{n}\left[1-(r\beta'+\beta)^n\right] = \frac{1}{n}\left[1-\beta^n(1+P)^n\right],$$

$$e_{\theta\theta} = e_{\varphi\varphi} = \frac{1}{n}[1-\beta^n]\ , \tag{2}$$

where: n is the measure; and $r\beta' = \beta P$; P is a function of β; and β is a function of radius.

Stress-strain relation: stress-strain relations for isotropic material, /28/, are:

$$T_{ij} = c_{ijkl}e_{kl}\ ,\quad (i,j,k,l = 1,2,3)\ ,$$

where: T_{ij} and e_{kl} are stress and strain tensors respectively. These nine equations contain a total of 81 coefficients e_{ijkl}, but not all the coefficients are independent. The symmetry of T_{ij} and e_{ij} reduces the number of independent coefficients to 36. For transversely isotropic materials which have a plane of elastic symmetry, these independent coefficients reduce to 5. The constitutive equations for transversely isotropic media are, /1/:

$$\begin{bmatrix} T_{11} \\ T_{22} \\ T_{33} \\ T_{23} \\ T_{31} \\ T_{12} \end{bmatrix} = \begin{bmatrix} c_{11} & c_{12} & c_{13} & 0 & 0 & 0 \\ c_{12} & c_{11} & c_{13} & 0 & 0 & 0 \\ c_{13} & c_{13} & c_{33} & 0 & 0 & 0 \\ 0 & 0 & 0 & c_{44} & 0 & 0 \\ 0 & 0 & 0 & 0 & c_{44} & 0 \\ 0 & 0 & 0 & 0 & 0 & \frac{1}{2}(c_{11}-c_{12}) \end{bmatrix} \begin{bmatrix} e_{11} \\ e_{22} \\ e_{33} \\ e_{23} \\ e_{31} \\ e_{12} \end{bmatrix}. \tag{3}$$

Substituting Eq.(2) in Eq.(3), we get

$$T_{rr} = \frac{c_{33}}{n}\left[1-(r\beta'+\beta)^n\right] + \frac{1}{n}(2c_{12})(1-\beta^n) \Rightarrow c_{33}e_{rr} + 2c_{12}e_{\theta\theta}\ ,$$

$$T_{\theta\theta} = T_{\varphi\varphi} = \frac{c_{21}}{n}\left[1-(r\beta'+\beta)^n\right] + \frac{2}{n}(c_{11}-c_{66})(1-\beta^n) \Rightarrow$$

$$\Rightarrow c_{12}e_{rr} + 2(c_{11}-c_{66})e_{\theta\theta}\ ,$$

$$T_{r\theta} = T_{\theta\varphi} = T_{\varphi r} = 0\ . \tag{4}$$

Equation of equilibrium: equations of equilibrium are:

$$\frac{\partial T_{rr}}{\partial r} + \frac{1}{r\sin\theta}\frac{\partial T_{r\varphi}}{\partial\varphi} + \frac{1}{r}\frac{\partial T_{r\theta}}{\partial\theta} + \frac{2T_{rr} - T_{\theta\theta} - T_{\varphi\varphi} + T_{r\theta}\cot\theta}{r} = 0\ ,$$

$$\frac{\partial T_{r\theta}}{\partial r} + \frac{1}{r\sin\theta}\frac{\partial T_{\theta\varphi}}{\partial\varphi} + \frac{1}{r}\frac{\partial T_{\theta\theta}}{\partial\theta} + \frac{3T_{r\theta} + (T_{\theta\theta} - T_{\varphi\varphi})\cot\theta}{r} = 0\ ,$$

$$\frac{\partial T_{r\varphi}}{\partial r} + \frac{1}{r\sin\theta}\frac{\partial T_{\varphi\varphi}}{\partial\varphi} + \frac{1}{r}\frac{\partial T_{\varphi\theta}}{\partial\theta} + \frac{3T_{r\varphi} + 2T_{\theta\theta}\cot\theta}{r} = 0\ . \tag{5}$$

Substituting Eq.(4) in Eq.(5), we see that the equations of equilibrium are all satisfied except:

$$\frac{\partial T_{rr}}{\partial r} + \frac{2T_{rr} - T_{\theta\theta} - T_{\varphi\varphi}}{r} = 0\ , \tag{6}$$

or

$$\frac{\partial T_{rr}}{\partial r} + \frac{2}{r}(T_{rr} - T_{\theta\theta}) = 0\ . \tag{7}$$

From Eq.(7), one may also say that

$$T_{\varphi\varphi} - T_{\theta\theta} = 0\ . \tag{8}$$

Equation (8) is satisfied by $T_{\theta\theta}$ and $T_{\phi\phi}$ as given by Eq.(2). If $c_{21} = c_{31}$, $c_{22} - c_{33} = c_{32} - c_{23}$, the equation of equilibrium from Eq.(6) becomes:

$$\frac{\partial T_{rr}}{\partial r} + \frac{2(T_{rr} - T_{\theta\theta})}{r} = 0\ . \tag{9}$$

Critical points or turning points: by substituting Eq.(4) into Eq.(9), we get a nonlinear differential equation in terms of β:

$$P(P+1)^{n+1}\beta\frac{dP}{d\beta} + P(P+1)^n + 2(1-C_1)P - \frac{2}{n\beta^n}(Q_1 - Q_2)\ , \tag{10}$$

$$Q_1 = C_1\left\{1-\beta^n(1-P)^n\right\},\quad Q_2 = C_2(1-C_1)(1-\beta^n)\ ,$$

$$C_1 = (c_{33}-c_{13})/c_{33} \quad \text{and} \quad C_2 = (c_{11}+c_{12}-2c_{13})/[c_{33}(1-C_1)]\ ,$$

where: P is function of β; and β is function of r only.

Transition points: transition points of β in Eq.(10) are $P = 0$, $P \to -1$, and $P \to \pm\infty$.

To solve the elastoplastic stress problems we consider the case of $P \to \pm\infty$.

Boundary condition: boundary conditions of the problem are given by:

$$r = a\ ,\quad \tau_{rr} = 0$$

$$r = b\ ,\quad \tau_{rr} = -p\ . \tag{11}$$

PROBLEM SOLUTION

For finding elastic-plastic stresses, the transition function is taken through the principal stresses at transition point $P \to \pm\infty$, we define the transition function ζ as:

$$\zeta = (3-2C_1) - \frac{nT_{rr}}{c_{33}} \cong \left[\beta^n (P+1)^n + 2(1-C_1)\right], \quad (12)$$

where: ζ is the transition function of r only. Taking the logarithmic differentiation of Eq.(12), with respect to r and using Eq.(10), we get

$$\frac{d(\log\zeta)}{dr} = \frac{-2C_1}{r}. \quad (13)$$

Taking the asymptotic value of Eq.(13) as $P \to \pm\infty$ and integrating, we get

$$\zeta = Ar^{-2C_1}, \quad (14)$$

where: A is a constant of integration; and $C_1 = (c_{33} - c_{13})/c_{33}$. From Eqs.(12) and (14), we have

$$T_{rr} = \frac{c_{33}}{n}\left[(3-2C_1) + Ar^{-2C_1}\right]. \quad (15)$$

Using boundary condition from Eq.(11) in Eq.(15), we get

$$A = -\frac{(3-2C_1)}{a^{-2C_1}} \text{ and } p = -\frac{c_{33}}{n}\left\{(3-2C_1)\left[1-\left(\frac{b}{a}\right)^{-2C_1}\right]\right\}. \quad (16)$$

Substituting Eq.(16) in Eq.(15), and using Eq.(16) in equation of equilibrium, we get

$$T_{rr} = \frac{c_{33}}{n}\left\{(3-2C_1)\left[1-\left(\frac{r}{a}\right)^{-2C_1}\right]\right\},$$

$$T_{\theta\theta} = T_{rr} + \frac{c_{33}}{n}\left[(3-2C_1)C_1\left(\frac{r}{a}\right)^{-2C_1}\right]. \quad (17)$$

Initial yielding: from Eq.(17) it is seen that $|T_{\theta\theta} - T_{rr}|$ is maximal at the outer surface, therefore, yielding of the shell will take place at the external surface of the shell:

$$\left|T_{\theta\theta} - T_{rr}\right|_{\substack{r=b \\ \text{(external} \\ \text{surface)}}} = \left|\frac{c_{33}}{n}\left[(3-2C_1)C_1\left(\frac{b}{a}\right)^{-2C_1}\right]\right| \equiv Y(\text{yielding}). \quad (18)$$

Using Eq.(18) in Eqs.(15)-(17), we get transitional stresses as in non-dimensional components:

$$\sigma_{rr} = \frac{1}{C_1}\frac{1-R^{-2C_1}}{R_0^{-2C_1}}, \quad \sigma_{\theta\theta} = \frac{1}{C_1}\frac{1-R^{-2C_1}}{R_0^{-2C_1}} + \frac{R^{-2C_1}}{R_0^{-2C_1}},$$

and

$$P_{oi} = \frac{R_0^{-2C_1} - 1}{C_1 R_0^{-2C_1}}, \quad (19)$$

where: $R = r/a$; $R_0 = b/a$; $\sigma_{rr} = T_{rr}/Y$; $\sigma_{\theta\theta} = T_{\theta\theta}/Y$; and $P_{oi} = p/Y$.

Fully plastic state: for the fully-plastic case, /24/, $C_1 \to 0$; therefore, stresses and pressure from Eq.(19) become:

$$\sigma_{rr} = 2Y^* \log R_0, \quad \sigma_{\theta\theta} = 2Y^* \log R, \text{ and } P_{of} = Y^* + \sigma_{rr}, \quad (20)$$

where: $R = r/a$; $R_0 = b/a$; $\sigma_{rr} = T_{rr}/Y^*$; $\sigma_{\theta\theta} = T_{\theta\theta}/Y^*$; and $P_{of} = p/Y^*$.

NUMERICAL RESULTS AND DISCUSSION

The above investigations elaborate the initial yielding and fully plastic state of crown made of zirconia and titanium modelled in form of hemispherical shell subjected to external pressure, to analyse uniaxial compression. The elastic constants for the same are taken from literature, /7, 11/, which are obtained by ultrasonic resonance spectroscopy, a non-destructive measure to obtain the stiffness constants. The results obtained for both types of crowns are compared with enamel and dentine. Enamel is made up of hydroxyapatite (HAP) mineral, 95 % by vol. All these materials exhibit transversely isotropic macrostructural symmetry.

In Fig. 2, the curves are plotted for pressure at initial yielding at various radius ratios. It is observed that intensity of pressure at initial yielding increases with increase in the thickness of the shell. It has been observed that titanium has the lowest yield strength and yields at lower levels of stress as compared to enamel and zirconia. Figures 3 and 4 show the trends of radial and circumferential stresses at initial yielding. Maximal stresses are observed at external surface of the shell. In Fig. 5, the curves are plotted for pressure required at fully plastic state for various radius ratios. It has been observed that shells exhibit high plasticity when the thickness of shell is between ratios $1 < R_0 < 3$, particularly zirconia. A significant drop in the levels of plasticity is observed when thickness increases. The plasticity of zirconia is inferred to be greater than that of titanium. Figures 6 and 7 represent the trends of radial and circumferential stresses at fully plastic state. The observations infer to the fact that principal stress differences are maximal at external surface of the crowns.

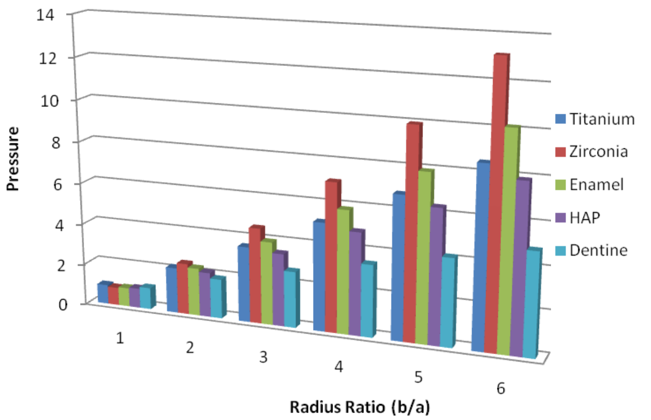

Figure 2. Pressure in the shell at initial yielding for radius ratio R_0.

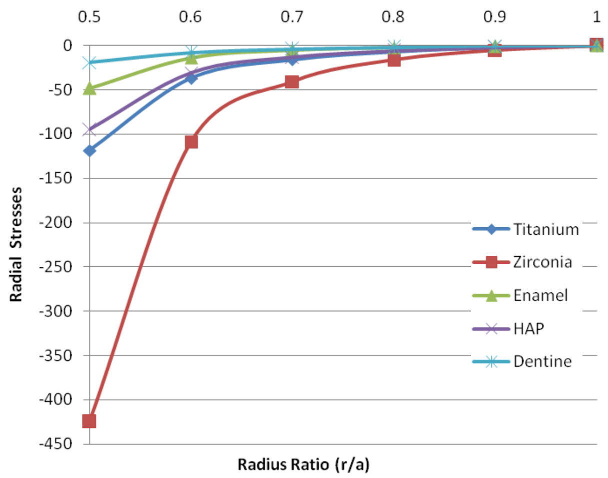

Figure 3. Radial stresses at initial yielding.

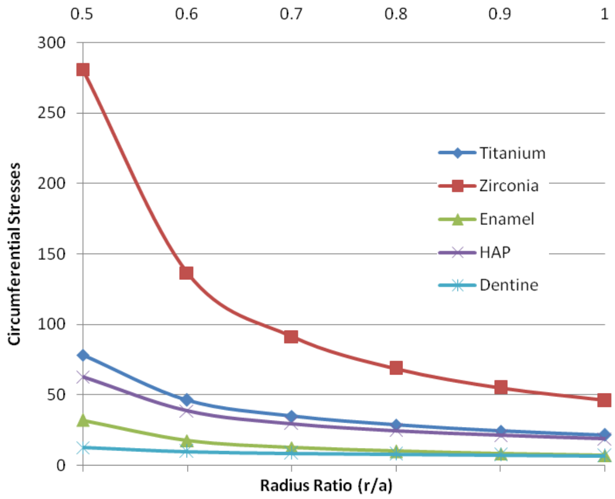

Figure 4. Circumferential stresses at initial yielding.

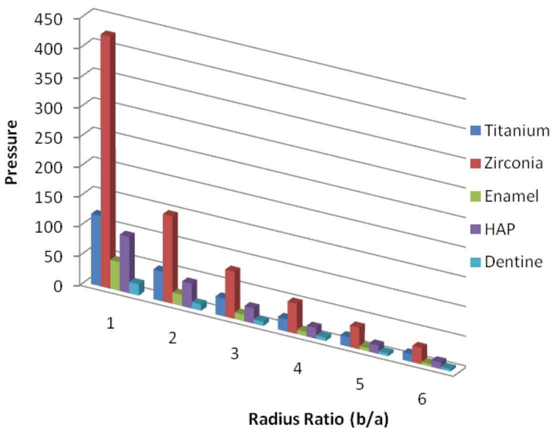

Figure 5. Pressure in the shell at fully plastic state for radius ratio R_0.

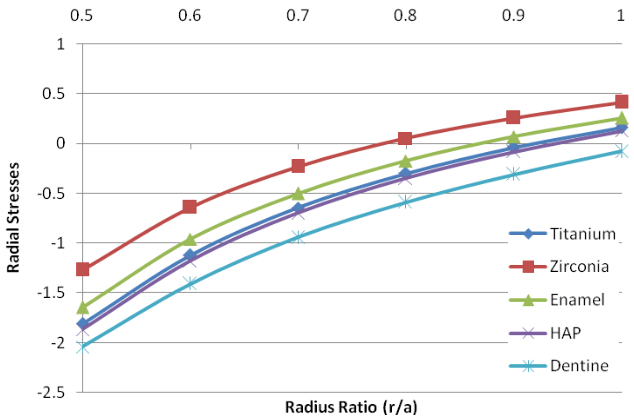

Figure 6. Radial stresses at fully plastic state.

CONCLUSIONS

We have investigated elastic-plastic transitional stress concentrations using Seth's transition theory for implants of molars and premolars modelled as hemispherical shells under external pressure. The findings allow us to conclude the following.

Zirconia has greater resemblance with enamel with necessary elastic and plastic limit, which demonstrates considerable ability to suppress crack growth.

Varying values of pressure required for initial yielding and fully plastic state are calculated for various radius ratios depending on the geometry of the crown sample. Trends on

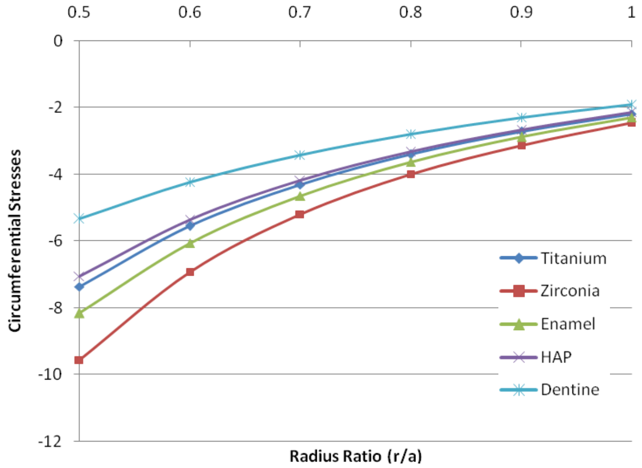

Figure 7. Circumferential stresses at fully plastic state.

the graphs are similar for enamel and hydroxyapatite due to enamel composition.

Significant difference between stress build-up at inner and outer layer of the implant crown is observed by varying the radii ratios.

REFERENCES

1. Altenbach, H., Altenbach, J., Kissing, W., Mechanics of Composite Structural Elements, Springer-Verlag, Berlin, Heidelberg, 2004. doi: 10.1007/978-3-662-08589-9
2. Bianchi, A.E., Bosetti, M., Dolci, G., et al. (2004), *In vitro and in vivo follow-up of titanium transmucosal implants with zirconia collar*, J Appl. Biomater. Biomech. 2(3): 143-150. doi: 10.1177/228080000400200303
3. Boyle, J.T., Spence, J., Stress Analysis for Creep, Butterworth-Heinemann, Elsevier Ltd., 1983. doi: 10.1016/C2013-0-00873-0
4. Cuy, J.L., Mann, A.B., Livi, K.J., et al. (2002), *Nanoindentation mapping of the mechanical properties of human molar tooth enamel*, Arch. Oral Biol. 47(4): 281-291. doi: 10.1016/s0003-9969(02)00006-7
5. Degidi, M., Artese, L., Scarano, A., et al. (2006), *Inflammatory infiltrate, microvessel density, nitric oxide synthase expression, vascular endothelial growth factor expression, and proliferative activity in peri-implant soft tissues around titanium and zirconium oxide healing caps*, J Periodontol. 77(1): 73-80. doi: 10.1902/jop.2006.77.1.73
6. Depprich, R., Ommerborn, M., Zipprich, H., et al. (2008), *Behavior of osteoblastic cells cultured on titanium and structured zirconia surfaces*, Head Face Med. 4: 29. doi: 10.1186/1746-160X-4-29
7. Menéndez-Proupin, E., Cervantes-Rodríguez, S., Osorio-Pulgar, R., et al. (2011), *Computer simulation of elastic constants of hydroxyapatite and fluorapatite*, J Mech. Behav. Biomed. Mater. 4(7): 1011-1020. doi.org/10.1016/j.jmbbm.2011.03.001
8. Fung, Y.C. (Ed.), Foundations of Solid Mechanics, Englewood Cliffs, N.J. Prentice-Hall, 1965.
9. Hallmann, L., Mehl, A., Ulmer, P., et al. (2012), *The influence of grain size on low-temperature degradation of dental zirconia*, J Biomed. Mater. Res. B Appl. Biomater. 100(2): 447-456. doi: 10.1002/jbm.b.31969
10. Inokoshi, M., Zhang, F., De Munck, J., et al. (2014), *Influence of sintering conditions on low-temperature degradation of dental zirconia*, Dent Mater. 30(6): 669-678. doi: 10.1016/j.dental.2014.03.005
11. Kinney, J.H., Balooch, M., Marshall, G.W., Marshall, S.J. (1999), *A micromechanics model of the elastic properties of human*

dentine, Arch. Oral Biol. 44(10): 813-822. doi: 10.1016/s0003-9969(99)00080-1

12. Kraus, H., Creep Analysis, J. Wiley & Sons, New York, 1980.
13. Liang, J.Z. (2002), *Toughening and reinforcing in rigid inorganic particulate filled poly(propylene): A review*, J Appl. Polym. Sci. 83(7): 1547-1555. doi: 10.1002/app.10052
14. Lubhan, D., Felger, R.P., Plasticity and Creep of Metals, Wiley, New York, USA, 1961.
15. Lughi, V., Sergo, V. (2010), *Low-temperature degradation - aging - of zirconia: A critical review of the relevant aspects in dentistry*, Dent. Mater. 26(8): 807-820. doi: 10.1016/j.dental.2010.04.006
16. Marshall, S.J., Balooch, M., Breunig, T., et al. (1998), *Human dentin and the dentin-resin adhesive interface*, Acta Mater. 46 (7): 2529-2539. doi: 10.1016/S1359-6454(98)80037-2
17. Muhammad, I.D., Awang, A., Mamat, O. (2014), *Modelling the elastic constants of cubic zirconia using molecular dynamics simulations*, Adv. Mater. Res. 845: 387-391. doi: 10.4028/www.scientific.net/AMR.845.387
18. Parkus, H., Thermoelasticity, Springer-Verlag, Wien, 1976. doi: 10.1007/978-3-7091-8447-9
19. Craig, R.G., Peyton, F.A., Johnson, D.W. (1961), *Compressive properties of enamel, dental cements, and gold*, J Dent. Res. 40(5): 936-945. doi: 10.1177/00220345610400051
20. Rimondini, L., Cerroni, L., Carrasi, A., Torricelli, P. (2002), *Bacterial colonization of zirconia ceramic surfaces: an in vitro and in vivo study*, Int. J Oral Maxillofac. Implants, 17(6): 793-798. PMID: 12507238
21. Scarano, A., Piatelli, M., Caputi, S., et al. (2004), *Bacterial adhesion on commercially pure titanium and zirconium oxide disks: an in vivo human study*, J Periodontol. 75(2): 292-296. doi: 10.1902/jop.2004.75.2.292
22. Seth, B.R. (1962), *Transition theory of elastic-plastic deformation, creep and relaxation*, Nature, 195: 896-897. doi:10.1038/195896a0
23. Seth, B.R. (1966), *Measure concept in mechanics*, Int. J Nonlinear Mech., 1(1): 35-40. doi: 10.1016/0020-7462(66)90016-3
24. Seth, B.R. (1963), *Elastic-plastic transition in shells and tubes under pressure*, J Appl. Math. Mech. (ZAMM), 43(7-8): 345-351. doi: 10.1002/zamm.19630430706
25. Shahi, S., Singh, S.B. (2020), *Elastic plastic transitional stress analysis of human tooth enamel and dentine under external pressure using Seth's transition theory*, In: S.B. Singh, A.V. Vakhrushev, A.K. Haghi, (Eds.), Materials Physics and Chemistry, Appl. Math. Chemo-Mech. Anal., Taylor & Francis Group, AAP. doi: 10.1201/9780367816094
26. Shahi, S., Singh, S.B., Thakur, P. (2019), *Modeling creep parameter in rotating discs with rigid shaft exhibiting transversely isotropic and isotropic material behavior*, J Emerg. Technol. Innov. Res. 6(1): 387-395.
27. Shahi, S., Singh, S.B., Kumar, P. (2021), *Mathematical modeling of elastic plastic transitional stresses in CNT-GS based hybrid nanocomposite thin walled spherical pressure vessels*, IOP Conf. Ser.: Mater. Sci. Eng. 1033: 012058. doi: 10.1088/1757-899X/1033/1/012058
28. Sokolnikoff, I.S., Mathematical Theory of Elasticity, 2nd Ed., McGraw-Hill Inc., New York, 1953.
29. Stanford, J.W., Weigel, K.V., Paffenbarger, G.C., Sweeney, W.T. (1960), *Compressive properties of hard tooth tissues and some restorative materials*, J Am. Dent. Assoc. 60: 746-756. doi: 10.14219/jada.archive.1960.0258
30. Stanford, J.W., Paffenbarger, G.C., Kumpula, J.W., Sweeney, W.T. (1958), *Determination of some compressive properties of human enamel and dentin*, J Am. Dent. Assoc. 57(4): 487-495. doi: 10.14219/jada.archive.1958.0194
31. Stawarczyk, B., Ozcan, M., Hallmann, L., et al. (2013), *The effect of zirconia sintering temperature on flexural strength, grain size, and contrast ratio*, Clin. Oral Investig. 17(1): 269-274. doi: 10.1007/s00784-012-0692-6
32. Thakur, P., Shahi, S., Singh, S.B., Sethi, M. (2019), *Elastic-plastic stress concentrations in orthotropic composite spherical shells subjected to internal pressure*, Struct. Integ. Life, 19(2): 73-77.
33. Thakur, P., Sethi, M., Shahi, S., et al. (2018), *Exact solution of rotating disc with shaft problem in the elastoplastic state of stress having variable density and thickness*, Struct. Integ. Life, 18(2): 128-134.
34. Thakur, P., Shahi, S., Gupta, N., Singh, S.B. (2017), *Effect of mechanical load and thickness profile on creep in a rotating disc by using Seth's transition theory*, AIP Conf. Proc., Amer. Inst. of Physics, USA, 1859(1): 020024. doi.org/10.1063/1.4990177
35. Timoshenko, S.P., Woinowsky-Krieger, S., Theory of Plates and Shells, 2nd Ed., McGraw-Hill, New York, 1959.
36. Zaytsev, D., Grigoriev, S., Panfilov, P. (2012), *Deformation behavior of human dentin under uniaxial compression*, Int. J Biomater. Art. ID: 854539. doi: 10.1155/2012/854539